World Academy of Science, Engineering and Technology
International Journal of Mechanical and Mechatronics Engineering
Vol:2, No:5, 2008

Optimal Speed Controller Design of the Two-Inertia Stabilization System

Byoung-Uk Nam, Hag-Seong Kim, Ho-Jung Lee, and Dong-Hyun Kim

***Abstract*—**This paper focuses on systematic analysis and controller design of the two-inertia STABILIZATION system, considering the angular motion on a base body. This approach is essential to the stabilization system to aim at a target under three or six degrees of freedom base motion. Four controllers, such as conventional PDF(Pseudo-Derivative Feedback) controller with motor speed feedback, PDF controller with load speed feedback, modified PDF controller with motor-load speed feedback and feedforward controller added to modified PDF controller, are suggested to improve reference tracking and disturbance rejection performance. Characteristics and performance of each controller are analyzed and validated by simulation in the case of the modified PDF controller with and without a feedforward controller.

***Keywords*—**Two-Inertia stabilization System, ITAE criterion, Speed Control.

I. Introduction

IN general motion control applications, the plant is composed of a motor, a geared transmission, and a load. A transmission device, which amplifies motor driving torque and reduces motor driving speed, is one of the essential elements to drive high inertia load by small inertia motor.

A two-inertia system, which consists of a motor, a gear, a flexible shaft and load, has low torsional resonant/anti-resonant frequency because of low stiffness in the flexible shaft. Therefore, system stiffness must be carefully designed during controller design, because the system bandwidth is extremely limited by the presence of a torsional resonance/anti-resonance of the mechanical system.

Numerous papers are conducted to obtain a better response from the two-inertia systems under the flexible shaft. Jang and Furusho applied three kinds of typical pole assignments with identical radius/damping coefficient/real part were applied by using a conventional proportional-integral speed control system[1]. This paper showed that only two adjustable feedback coefficients are not sufficient to arbitrarily assignment four poles. An observer-based state feedback compensator for major control loop was proposed[2]. The features of this control scheme yielded a robust system with respect to system uncertainties and modeling errors and showed very effective results for the vibration suppression. By analyzing the dominant properties at low and high frequency region, a simple magnitude shaping design was developed using ITAE(Integral of Time multiplied by the Absolute Error) index, and a relationship between the anti-resonance and resonance magnitude was deduced[3]. The Kalman filter and LQ-based speed controller for torsional vibration suppression was also presented [4]. In [5], three kinds of speed controller(I-P, I-PD, and State Feedback) were compared to provide a systematic analysis and a introduced design of a pole placement controller by using the weighted ITAE performance index for a two-inertia motor system.

These previous researches based on the two-inertia system model have not considered the angular base motion. In practical of view, many control platforms should have stabilization capabilities to aim at a target under three or six degrees of freedom base motions. However, only few papers have been reported on systematic analysis and controller design for the two-inertia STABILIZATION system, considering the angular base motion.

In this paper, the systematic analysis of two-inertia stabilization system is proposed, and an optimal controller to achieve better reference tracking and disturbance rejection performance is introduced by pole assignment using ITAE criterion. In order to improve the disturbance rejection performance, a feedforward controller is suggested and compared with non-feedforward controller.

II. System Modelling

A. Two-Inertia System Model

The general configuration of a two-inertia system, which comprises gear box mechanism, is shown in Fig. 1. Its simplified block diagram is also shown in Fig. 2, ignoring nonlinearities such as backlash, damping, and friction.

Open loop transfer function is given by (1), from motor torque to motor speed, and (2), from motor torque to load speed [6].

$$\frac{\dot{\theta}_m(s)}{T_m} = \frac{1}{NJ_{meq}s}\frac{s^2+\omega_z^2}{s^2+\omega_p^2} \quad (1)$$

$$\frac{\dot{\theta}_l(s)}{T_m} = \frac{1}{J_{meq}s}\frac{\omega_z^2}{s^2+\omega_p^2} \quad (2)$$

Manuscript received April 28, 2008

B. U. Nam is working on Automotive & Armament Directorate, 5th R&D Institute, Agency for Defense Development, Yuseong P.O.Box 35-5, Daejeon, Korea (e-mail: nbu@ add.re.kr).

H. S. Kim, H. J. Lee and D. H. Kim are working on Automotive & Armament Directorate, 5th R&D Institute, Agency for Defense Development, Yuseong P.O.Box 35-5, Daejeon, Korea.

$$\omega_z = \sqrt{\frac{K_{eq}}{J_l}}, \quad \omega_p = \omega_z \sqrt{1 + \frac{J_l}{J_{meq}} \frac{1}{N^2}} \tag{3}$$

In (1) and (2), anti-resonant(ω_z) and resonant(ω_p) frequencies are given by (3), respectively.

Control bandwidth(ω_c) is generally limited by the anti-resonance of the mechanical system in closed loop motion control system. Therefore, higher mechanical stiffness of the shaft is required to increase the control bandwidth. Equation (4) shows the minimum required mechanical stiffness, which can be described by the desired control bandwidth and load inertia.

$$K_{eq} > \omega_c^2 J_l \tag{4}$$

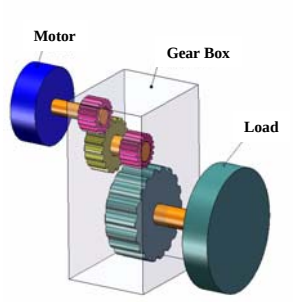

Fig. 1 General configuration of the motor drive system

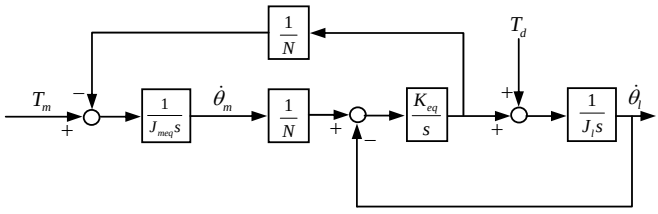

Fig. 2 Linearized block diagram of a two-inertia system

T_m : *Motor Input Torque*, T_d : *Disturbance Torque*
J_m : *Motor Inertia*, J_{meq} : *Motor Inertia with Gear Box*
J_l : *Load Inertia*, J_{eq} : *Equivalent System Inertia*
$\dot{\theta}_m$: *Motor Speed*, $\dot{\theta}_l$: *Load Speed*
$\dot{\theta}_h$: *Angular Disturbance Speed*
N : *System Gear Ratio*
K_{eq} : *Torsional Stiffness of the Shaft*

B. Two-Inertia Stabilization System Model

In practical of view, many control platforms in military region, especially the gun/turret stabilization system and marine satellite antenna stabilization system, should guarantee stabilization capability to aim at a target under three or six degrees of freedom base motions. Therefore, a proper system model considering angular base motion is required to design an optimal controller, which is named two-inertia stabilization system model in this paper. The two-inertia stabilization system model is shown in Fig. 3. The angular base motion is added to the two-inertia system model (shown in Fig. 2) and coupled into the load motion because of the kinematics of a gear driven system.

Open loop transfer functions of the two-inertia stabilization system are equal to that of two-inertia system, shown in (1), from motor torque to motor speed, and (2), from motor torque to load speed.

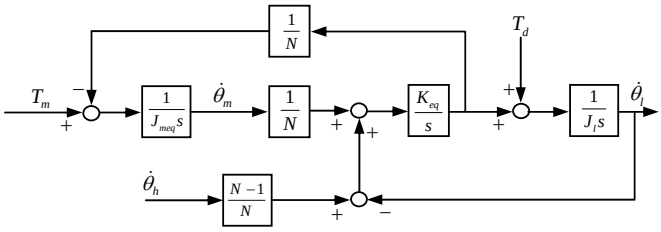

Fig. 3 Linearized block diagram of a two-inertia stabilization system

III. Analysis and Design of the Controllers

In this section, we propose four types of speed controllers for two-inertia stabilization system to achieve a better speed response to suppress the mechanical vibrations and to have a better angular command tracking and angular disturbance rejection performance

First, a conventional PDF(Pseudo-Derivative Feedback) controller with motor speed feedback[1],[3],[5], which is generally applied to two-inertia system in industrial field, is applied for two-inertia stabilization system.

Second, a PDF controller with load speed feedback is suggested for better angular disturbance performance.

Next, modified PDF controller with motor and load speed feedback is suggested to assign closed-loop poles by using the ITAE(Integral of Time multiplied by the Absolute Error) criterion [7], which assists in selecting optimal closed-loop poles to reduce oscillation. Generally, in stabilization system, angular load speed can be acquired by the gyroscope sensor.

Finally, a feedforward controller using angular speed data of the base motion is added to modified PDF controller for excellent angular disturbance rejection performance.

Characteristics and performances of each controller will be described to the following section.

A. General PDF Controller with Motor Speed Feedback

A block diagram of the speed control system using conventional PDF controller with motor speed feedback is shown in Fig. 4.

In Fig. 4, K_P is the proportional feedback gain of motor speed, K_I is the integral feedback gain of motor speed, and $\dot{\theta}_{cmd}$ is the speed command.

Closed-loop transfer functions of Fig. 4 are given by (5), from speed command to load speed, and (6), from disturbance speed to load speed.

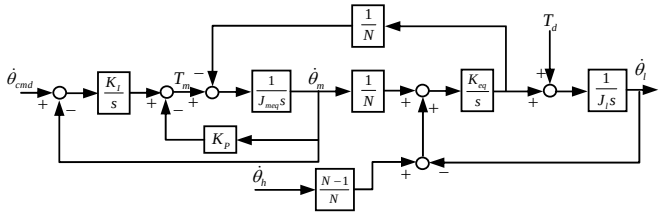

Fig. 4 Speed control system using conventional PDF controller with motor speed feedback

$$\frac{\omega_l(s)}{\omega_{cmd}(s)} = \frac{1}{N}\frac{K_I\omega_z^2}{J_{meq}s^2(s^2+\omega_p^2)+(K_Ps+K_I)(s^2+\omega_z^2)} \tag{5}$$

$$\frac{\omega_l(s)}{\omega_h(s)} = \frac{K_{eq}}{J_l}\frac{J_{meq}s^2+K_Ps+K_I}{J_{meq}s^2(s^2+\omega_p^2)+(K_Ps+K_I)(s^2+\omega_z^2)} \tag{6}$$

At (5), speed command tracking performance can be improved by proper gain tuning, but at (6), we can recognize that it is impossible to achieve good angular disturbance rejection by gain tuning in low frequency region [6],[8].

Now, it has verified that the conventional PDF controller with motor speed feedback is not appropriate to apply to the two-inertia stabilization system because of its weak disturbance rejection performance. Therefore, we suggest a PDF controller with load speed feedback.

B. PDF Controller with Load Speed Feedback

A block diagram of speed control system using a PDF controller with load speed feedback is shown in Fig. 5.

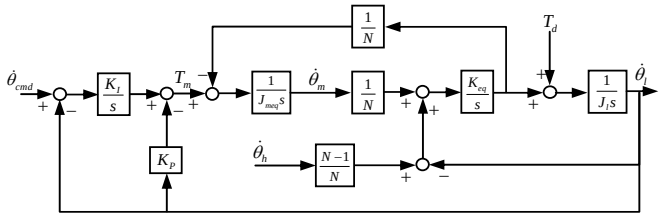

Fig. 5 Speed control system using PDF controller with load speed feedback

In Fig. 5, K_P is the proportional feedback gain of load speed, K_I is the integral feedback gain of load speed, and $\dot{\theta}_{cmd}$ is the speed command.

Closed-loop transfer functions of Fig. 5 can be formulated by (7) and (8).

$$\frac{\omega_l}{\omega_{cmd}} = \frac{K_I\omega_z^2}{NJ_{meq}s^2(s^2+\omega_p^2)+\omega_z^2(K_Ps+K_I)} \tag{7}$$

$$\frac{\omega_l}{\omega_h} = \frac{(N-1)J_{meq}\omega_z^2s^2}{NJ_{meq}s^2(s^2+\omega_p^2)+\omega_z^2(K_Ps+K_I)} \tag{8}$$

At (8), we can verify +40dB/decade angular disturbance rejection performance at low frequency region (related figure is shown in Fig. 8. (b)). However, it is difficult to design a precise controller because we have only two design parameters (K_P, K_I) whose number is less than the order of the system. Therefore, it's impossible to design a closed-loop pole assignment type controller by using conventional ITAE criterion.

Also, from the characteristic equation (9), we can figure out that the closed-loop control system is not stable through Routh's Stability Criterion [6], because there are two sign changes at Routh array shown by (10).

$$\begin{aligned} D(s) &= NJ_{meq}s^4 + NJ_{meq}\omega_p^2s^2 + \omega_z^2K_Ps + \omega_z^2K_I \\ &= NJ_{meq}s^4 + \varepsilon s^3 + NJ_{meq}\omega_p^2s^2 + \omega_z^2K_Ps + \omega_z^2K_I \\ &= a_4s^4 + a_3s^3 + a_2s^2 + a_1s^1 + a_0 \end{aligned} \tag{9}$$

$$\begin{aligned} a_4 &= NJ_{meq} > 0 \\ a_3 &= \varepsilon > 0 \\ b_1 &= \frac{1}{\varepsilon}(\varepsilon NJ_{meq}\omega_p^2 - NJ_{meq}\omega_z^2K_P) < 0 \\ c_1 &= \frac{1}{\varepsilon\omega_p^2 - \omega_z^2K_P}(-\frac{\omega_z^2K_I}{NJ_{meq}}\varepsilon^2 + \omega_p^2\omega_z^2K_P\varepsilon - \omega_z^4K_P^2) > 0 \\ d_1 &= \omega_z^2K_I > 0 \end{aligned} \tag{10}$$

In following section, we will propose a modified PDF controller with motor and load speed feedback to design Pole Assignment controller by using ITAE Criterion, that will guarantee stability and performance.

C. Modified PDF Controller with Motor- Load Speed Feedback

The block diagram of a control system using Modified PDF controller with motor-load speed feedback is shown in Fig. 6.

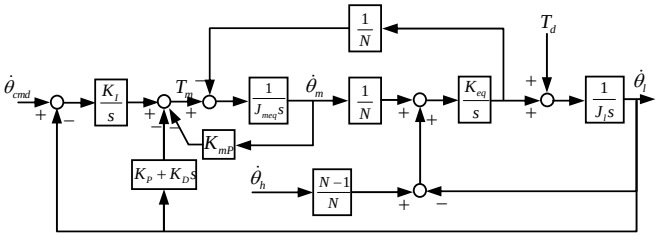

Fig. 6 Speed control system using modified PDF controller with motor-load speed feedback

In Fig. 6, K_{mP} is the proportional feedback coefficient of motor speed and K_D is the derivative feedback coefficient of load speed.

Closed-loop transfer functions of Fig. 6 can be described by (11) and (12)

$$\frac{\omega_l}{\omega_{cmd}} = \frac{K_I\omega_z^2}{NJ_{meq}s^4 + NK_{mP}s^3 + (NJ_{meq}\omega_p^2 + \omega_z^2K_D)s^2 + \omega_z^2(NK_{mP}+K_P)s + \omega_z^2K_I} \tag{11}$$

$$\frac{\omega_l}{\omega_h} = \frac{(N-1)\omega_z^2s(J_{meq}s+K_{mP})}{NJ_{meq}s^4 + NK_{mP}s^3 + (NJ_{meq}\omega_p^2 + \omega_z^2K_D)s^2 + \omega_z^2(NK_{mP}+K_P)s + \omega_z^2K_I} \tag{12}$$

Now, in the reference to output transfer function (11), all

coefficients of the characteristic equation can be determined for optimal pole assignment by ITAE Criterion to achieve a fast response, minimal overshoot, and better disturbance rejection. In (11), zero is not introduced in the closed-loop system when locations of poles are changed by pole assignment. This is very useful in minimum phase plant.

In (12), +20dB/decade angular disturbance rejection performance can be validated at low frequency region (related figure is shown in Fig. 8. (b)). We can notice that the DC value of angular disturbance rejection at zero frequency is determined by the integral gain (K_I) in (12), which also has effect on the closed-loop bandwidth. As stated in the previous section, to increase the integral value, mechanical stiffness has to be enhanced.

D. PDF Controller with motor- load speed feedback and feedforward controller

If a angular disturbance on a base body is measured, this signal can be used to reduce the effect of that disturbance on the output of the control system. A block diagram showing how feedforward controller using angular disturbance signal is implemented is shown in Fig. 7. In this block diagram, a disturbance feedforward controller is added to the modified PDF controller with motor-load speed feedback.

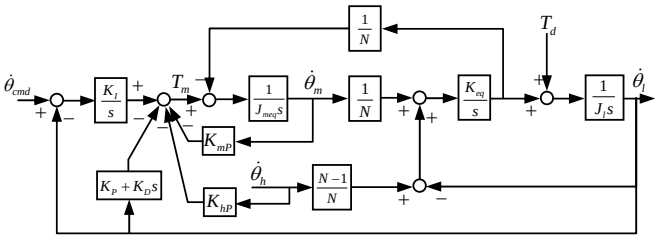

Fig. 7 Speed control system using modified PDF controller with motor-load speed feedback and feedforward Controller

In Fig. 6, K_{hP} is the proportional feedforward coefficient of disturbance speed.

Closed-loop transfer functions of Fig. 7 can be described by (13) and (14)

$$\frac{\omega_l}{\omega_{cmd}} = \frac{K_I\omega_z^2}{NJ_{meq}s^4 + NK_{mP}s^3 + (NJ_{meq}\omega_p^2 + \omega_z^2K_D)s^2 + \omega_z^2(NK_{mP} + K_P)s + \omega_z^2K_I} \quad (13)$$

$$\frac{\omega_l}{\omega_h} = \frac{(N-1)\omega_z^2 s(J_{meq}s + K_{mP} - \frac{K_{hP}}{N-1})}{NJ_{meq}s^4 + NK_{mP}s^3 + (NJ_{meq}\omega_p^2 + \omega_z^2K_D)s^2 + \omega_z^2(NK_{mP} + K_P)s + \omega_z^2K_I} \quad (14)$$

In Fig. 6 and Fig. 7, the reference to output transfer function and closed-loop characteristic equation are equal, because the feedforward controller does not affect closed-loop poles. In (14), angular disturbance rejection performance can be improved by tuning the feedforward gain(K_{hP}) : +40dB/decade angular disturbance rejection performance can be guaranteed at low frequency region (related figure is shown in Fig. 8. (b)).

IV. Simulation

In this section, simulation and verification of the modified PDF controller is carried out on a two-inertia stabilization system model. Especially, the reference tracking and disturbance rejection performance of proposed controllers, which is modified PDF controller with and without feedforward controller, are evaluated.

Simulations are carried out for different shaft stiffness, which has different closed-loop bandwidth. The proposed controller gains are determined by using ITAE criterion.

A. Plant and Disturbance Description

Load and disturbance specifications used in simulations are shown in Table I. In this case, gear inertia is included to motor inertia.

TABLE I
Parameter of System and Disturbance

Parameter		CASE 1	CASE 2
System Parameters	Motor Inertia with gear box $[Kgm^2]$	1.74×10^{-5}	1.74×10^{-5}
	Load Inertia $[Kgm^2]$	2.32	2.32
	Torsional Stiffness $[Nm/rad]$	1000	2000
	Gear Ratio	200	200
Disturbance Parameters	Angular speed amplitude[deg/s]	30	30
	Angular speed frequency[Hz]	0.5	0.5

B. Optimization of the Coefficients by ITAE Criterion

Optimal coefficients for the ITAE criterion are given by (15). The coefficients that will minimize the ITAE performance criterion for a step input have been determined for the general closed-loop transfer function.

$$\begin{aligned}
&s + \omega_n \\
&s^2 + 1.4\omega_n s + \omega_n^2 \\
&s^3 + 1.75\omega_n s^2 + 2.15\omega_n^2 s + \omega_n^3 \\
&s^4 + 2.1\omega_n s^3 + 3.4\omega_n^2 s^2 + 2.7\omega_n^3 s + \omega_n^4 \\
&s^5 + 2.8\omega_n s^4 + 5.0\omega_n^2 s^3 + 5.5\omega_n^3 s^2 + 3.4\omega_n^4 s + \omega_n^5 \\
&s^6 + 3.25\omega_n s^5 + 6.60\omega_n^2 s^4 + 8.60\omega_n^3 s^3 + 7.45\omega_n^4 s^2 + 3.95\omega_n^5 s + \omega_n^6
\end{aligned} \quad (15)$$

The gains of the controller obtained from ITAE criterion followers:

$$\begin{aligned}
K_P &= \frac{NJ_{meq}\omega_n(2.7\omega_n^2 - 2.1\omega_z^2)}{\omega_z^2} \\
K_D &= \frac{NJ_{meq}(3.4\omega_n^2 - \omega_p^2)}{\omega_z^2} \\
K_{mP} &= 2.1J_{meq}\omega_n \\
K_I &= \frac{NJ_{meq}\omega_n^4}{\omega_z^2} \\
K_{hP} &= 2.1(N-1)J_{meq}\omega_n
\end{aligned} \quad (16)$$

At Table I, the mechanical anti-resonant frequency exist at 3.3Hz(CASE I) and 4.67Hz(CASE II), so the closed-loop bandwidth was limited at 3Hz(CASE I) and 4.5Hz(CASE II) determining final controller gains.

C. *Analysis of Simulation Result*

The bode diagrams of reference tracking and disturbance rejection performance are shown in Fig. 8 and Fig.9, that its gains were determined by (16). In simulation, gravity effect and nonlinearities such as backlash, damping, and friction was neglected. And the sampling period of controller is set equal to 0.005 sec.

As stated at the previous section, we can obtain higher closed-loop bandwidth from 3Hz to 4.5Hz shown in Fig. 8 (a) and Fig. 9 (a) by enhancing stiffness of the shaft, and angular disturbance rejection performance was improved from +20dB/decade rejection ratio to +40dB/decade rejection ratio at low frequency region by adding a feedforward controller shown in Fig. 8 (b) and Fig. 9 (b).

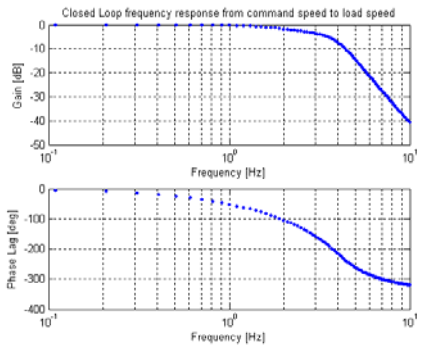

(a) Reference tracking

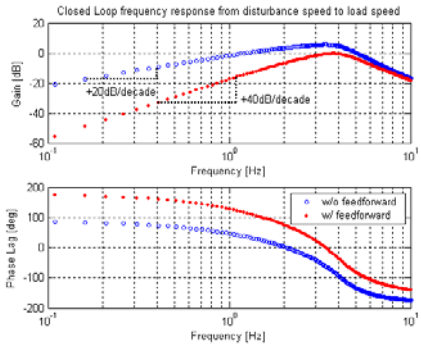

(b) Disturbance rejection

Fig. 8 Bode Plots at 3Hz bandwidth

The reference tracking responses using optimal coefficients by 3Hz and 4.5Hz ITAE criterion for 1rad/s step input are shown in Fig. 10. The overshoot and oscillation are small and the rising time is faster at coefficients by 4.5Hz ITAE criterion by enhancing mechanical stiffness.

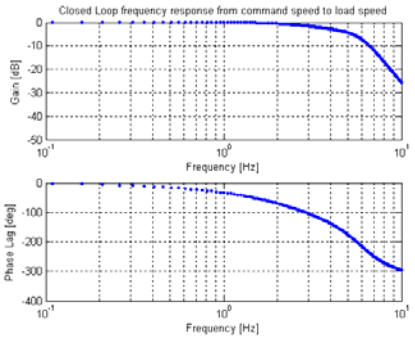

(a) Reference tracking

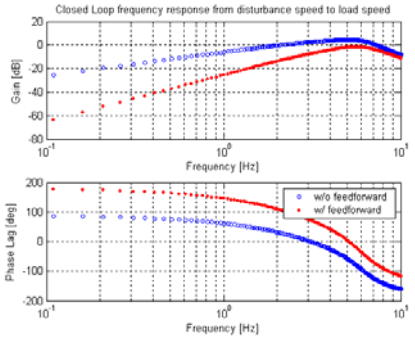

(b) Speed disturbance rejection

Fig. 9 Bode Plots at 4.5Hz Bandwidth

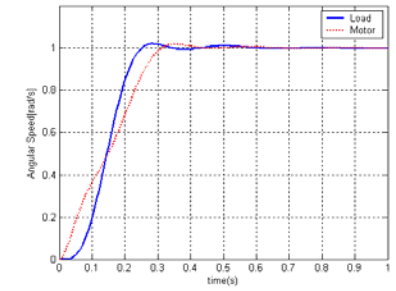

(a) 3Hz bandwidth

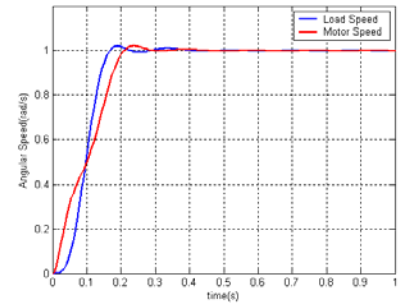

(b) 4.5Hz bandwidth

Fig. 10 Simulation results of reference tracking response

Disturbance rejection responses using optimal coefficients by 3Hz and 4.5Hz ITAE criterion for a 30deg/s and 0.5Hz sinusoidal disturbance are shown in Fig. 11. At Fig. 11 (a), -7.4dB disturbance rejection occurs without feedforward and

-29.2dB rejection occurs with feedforward. At Fig. 11 (b), -11.9dB disturbance rejection occurs without feedforward and -37.2dB rejection occurs with feedforward. Therefore, in disturbance rejection respect, adding feedforward controller is more effective to improve system performance rather than enlarge controller bandwidth with enhancing stiffness.

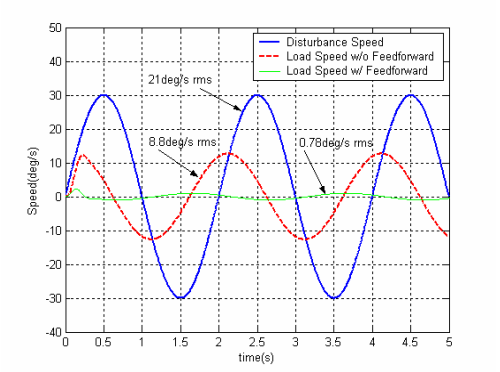

(a) 3Hz bandwidth

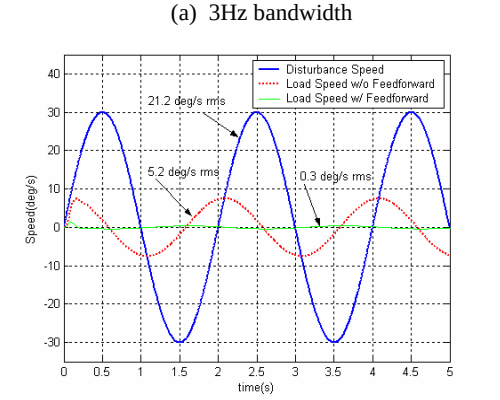

(b) 4.5Hz bandwidth

Fig. 11 Simulation results of disturbance rejection response

Therefore, we can design an optimal controller with respect to command tracking and disturbance rejection for two-inertia stabilization system by using previous controller design approach.

V. Conclusion

This paper suggested an optimum speed controller for better reference tracking and disturbance rejection performance for two-inertia stabilization system. The pole assignment is conducted by using ITAE criterion so that control system response was improved. The reference tracking performance was able to be improved at high frequency bandwidth by enhancing mechanical stiffness. On the other hand, the disturbance rejection performance enabled to be easily improved by adding feedforward controller. Therefore, the proposed design approach and result might provide a good controller design guideline for two-inertia stabilization system.

References

[1] G. Zang and J. Furusho, "Speed Control of Two-Inertia System by PI/PID Control," *IEEE Trans. Industrial Electronics*, vol.47, No.3, June 2000, pp. 603-609.

[2] R. Dhaouadi, K. Kubo, and M. Tobise, "Two-Degree-of-Freedom Robust Speed Controller for High-Performance Rolling Mill Drives," *IEEE Trans. on Industry Applications*, vol.29, No.5, September/ October 1993, pp. 919-926.

[3] G. Zang, J. Furusho, and M. Kajitani "A New Design Method of Servo Drive System with Torsional Load," in *Proc. IEEE IECON'98*, 1998, pp. 1114-1119.

[4] J. K. Ji and S. K. Sul, "Kalman filter and LG Based Speed Controller for Torsional Vibration Suppression in a 2-Mass Motor Drive System," *IEEE Trans. Industrial Electronics*, vol.IE-43, No.6, December 1995, pp. 564-571.

[5] G. Suh, D. S. Hyun, and J. I. Park, "Design of a Pole Placement Controller for Reducing Oscillation and Settling Time in a Two-Inertia Motor System," in *Proc. IEEE IECON'01*, 2001, pp. 615-620.

[6] G F. Franklin, J. D. Powell, A. Emami-Naeini, Feedback Control of Dynamic Systems 4th Edition, Prentice-Hall Inc., Upper Saddle River, NJ, 2002.

[7] R. C. DORF and R. H. BISHOP, Modern Control Systems 9th Edition, Prentice-Hall Inc., Upper Saddle River, NJ, 2001.

[8] K. OGATA, Modern Control Engineering 3rd Edition, Prentice-Hall Inc., Upper Saddle River, NJ, 1997.